Effect of Charge Mobility on Electric Conduction Driven Dielectric Liquid Flow

Miad Yazdani and Jamal Seyed-Yagoobi, *Senior Member, IEEE*

***Abstract*—Electrohydrodynamic (EHD) conduction pumping is associated with the heterocharge layers of finite thickness in the vicinity of the electrodes, generated by the process of dissociation of the neutral electrolytic species and recombination of the generated ions. EHD conduction generated flow relies primarily upon the asymmetry of the electrodes where the flow is always directed toward the specific direction regardless of the electrodes polarity. However, the difference in the mobilities of positive and negative charges could play an important role when studying the pumping performance. This paper studies the effects of charge mobility and its difference between the positive and negative charges on the heterocharge layer structure and generated flow. The numerical simulation is conducted for a 2-D rectangular channel with the electrodes embedded against the channel wall. The net flow generated for the symmetric electrodes is physically illustrated while the impact of mobility difference on the generated flow for the case of asymmetric electrodes is studied as well.**

***Index Terms*—EHD Conduction, dissociation and recombination, charge mobility.**

NOMENCLATURE

$b_{+/-}$	positive/negative charge mobility coefficient
b_r	mobility ratio, $b_r = b_+/b_-$
D	charge diffusion constant
d	channel half height
C_0	EHD dimensionless number
e	electron charge
$\mathbf{E}$	electric field vector
$\|\mathbf{E}\|$	electric field vector magnitude
$F(\omega)$	$I_1(2\omega)/\omega$
$I_1(z)$	modified Bessel function of first type and order one
k_B	Boltzmann universal constant
k_d	dissociation rate constant
k_r	recombination rate constant
n	negative charge density
$\mathbf{n}$	unit normal vector
p	positive charge density
P	pressure
$\mathrm{Re}_{\mathrm{ehd}}$	EHD Reynolds number
T_{sat}	saturation temperature
$\mathbf{u}$	velocity vector
u_{ehd}	EHD reference velocity
$\|\mathbf{u}\|$	velocity vector magnitude
V	applied electric potential
$\mathrm{Y_w}$	channel wall thickness
α	dimensionless charge diffusion constant
ϵ	absolute electric permittivity
η	electrode gap
μ	dynamic viscosity of fluid
ν	kinematic viscosity of fluid
ξ	electrode width
ξ_r	ground to HV electrode width, $\xi_r = \xi_g/\xi_{HV}$
ω	dissociation rate coefficient, $\omega = [\frac{e^3\|E\|}{4\pi\epsilon {k_B}^2 T_{sat}}]^{1/2}$
ρ	mass density
σ	electric conductivity of fluid
ϕ	potential field

SUBSCRIPTS

eq	equilibrium
g	ground electrode
HV	high voltage electrode

SUPERSCRIPT

$*$	dimensionless variable

I. INTRODUCTION

The EHD pumping phenomena involve the interaction of electric fields and flow fields in a dielectric fluid medium. This interaction between electric and flow fields induces the fluid motion through the presence of electric body force. EHD conduction pumping is associated with the heterocharge layers of finite thickness in the vicinity of the electrodes that are based on the process of dissociation of the neutral electrolytic species and recombination of the generated ions [1], [2]. The conduction term here represents a mechanism for electric current flow in which charged carriers are produced not by injection from the electrodes, but by dissociation of molecules within the fluid.

Feng and Seyed-Yagoobi [3] conducted an asymptotic analysis to study the effects of flow convection on the EHD conduction pumping and the associated energy transport. The EHD conduction driven flow rely primarily upon the asymmetry of the electrodes. The electrodes asymmetry results in the dominance of electric body force and flow generation in one direction. Yazdani and Seyed-Yagoobi [4] showed that the flow generation is always from the narrower electrode toward the wider electrode regardless of their polarity. They also showed that symmetric charge and body force distributions

Manuscript received April 17, 2009. This work was financially supported by the NASA Microgravity Fluid Physics Program.

M. Yazdani is currently PhD student with the Two Phase Flow and Heat Transfer Enhancement Laboratory in Mechanical, Materials and Aerospace Engineering Department, Illinois Institute of Technology, Chicago, IL, 60302 (email: myazdan1@iit.edu).

J. Seyed-Yagoobi is IEEE senior member and professor and chair of the Mechanical, Materials and Aerospace Engineering Department, Illinois Institute of Technology, Chicago, IL, 60302 (email: yagoobi@iit.edu).

over identical electrodes result in zero net flow generation when the charges have identical properties. However, recent experimental study by Hanaoka et. al [5] revealed that there exists a net generated flow in the case of symmetric electrodes configuration. Assuming that the diffusion has negligible effect on the charge distribution in macro-scales, the charge distribution symmetry over the identical electrodes could be broken only if the charges have different mobilities. There exist a limited number of publications focusing on the mobility measurements in dielectric liquids. Winkur et. al [6] conducted an experiment to measure the ion mobility in n-hexane and a $0.22M$ solution of biphenyl in n-hexane using a time-of-flight technique. This technique was used in several measurements of the mobility of positive ions in hydrocarbons (see for example [7] and references therein) with the discrepancies mainly raised by the methods of measurements. Huang and Freeman [8] measured the mobility of positive ions in liquid hydrocarbons and investigated the effects of density and temperature. They claimed that the positive ions mobility does not obey Walden's rule ($b_+ \propto \mu^{-1.0}$) but rather has a nonlinear relationship to the viscosity, $b_+ \propto \mu^{-1.2\pm0.1}$ as found earlier for ions in ethers. The time of flight method is later used by Sakamoto and Yamada [9] to study the ion mobilities and breakdown processes in dielectric liquids with razor-blade emitter grid collector used for the electrodes. They reported the streaming velocities for positive and negative agents in different liquids. Similar technique was used by Casanovas et. al [10] to measure the mobility of positive and negative ions in polydimethylsiloxane silicone oil.

The current study extends the fundamental study by Yazdani and Seyed-Yagoobi [4] to illustrate the role of charge mobility on the performance and characteristics of EHD conduction driven liquid flow. In particular, the impact of unequal mobilities for positive and negative charges on the generated flow for the case of symmetric electrodes is investigated and physically analyzed. This study is also extended to include the case of asymmetric electrodes where net flow is expected due to the electrodes asymmetry even in the case of equal mobilities for positive and negative carriers.

II. Theoretical Model

The theoretical model presented here is adopted from the model developed by Atten and Seyed-Yagoobi [11]. Their theoretical model was developed and solved analytically in the absence of any fluid motion assuming that the positive and negative charges possess identical mobilities. Jeong et al. [12] applied Atten and Seyed- Yagoobi's model to a complex electrode geometry and provided numerical solutions in the absence of fluid motion as well. The model presented in this section is based on the assumption that the dielectric liquid is incompressible and single phase with no contribution of charge injection from the electrodes' surfaces. The positive and negative charge mobilities are different which is the major departure of this paper from previous studies. It is assumed that the charge diffusion for positive and negative ions is constant and identical.

The schematic of the numerical domain for a symmetric electrode configuration is presented in Fig. 1. Table I presents

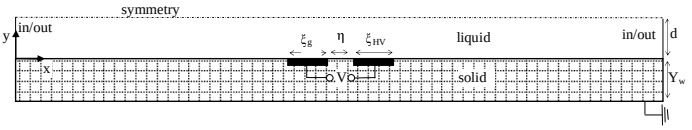

Fig. 1. Schematic of numerical domain (not to scale). Detail of the electrodes design is provided in Table I.

TABLE I
DETAILS OF THE ELECTRODES DESIGNS CHARACTERISTICS. ALL DIMENSIONS ARE NORMALIZED WITH THE CHANNEL HALF HEIGHT, $d = 2mm$

Electrodes Configuration	Channel wall thickness (mm)	Ground electrode (mm)	HV electrode (mm)	Electrode gap (mm)
Symmetric	Y_w = 4 (Y_w^* = 2)	ξ_g = 2 (ξ^*_g = 1)	ξ_{HV} =2 (ξ^*_{HV} = 1)	η = 1 (η^* = 0.5)
Asymmetric, ξ_r = 0.35		ξ_g = 0.7 (ξ^*_g = 0.35)	ξ_{HV} =2 (ξ^*_{HV} = 1)	
Asymmetric, ξ_r = 2.86		ξ_g = 2 (ξ^*_g = 1)	ξ_{HV} =0.7 (ξ^*_{HV} = 0.35)	

the details of the electrode design for symmetric and asymmetric electrodes configurations.

In steady-state, the system described here is governed by the following equations.

$$\nabla \cdot \mathbf{u} \tag{1}$$

$$\mathbf{u} \cdot \nabla \mathbf{u} = -\frac{1}{\rho}\nabla P + \nu \nabla^2 \mathbf{u} + (\rho_+ - \rho_-)\mathbf{E} \tag{2}$$

The last term on the left hand side of equation. (2) is the electric body force and should be obtained by solving the Maxwell's relation and charge transport equations:

$$\nabla \cdot \mathbf{E} = \frac{(p-n)}{\epsilon}; \quad \mathbf{E} = -\nabla\phi \tag{3}$$

$$\nabla \cdot \left[\begin{pmatrix} b_+ p \\ -b_- n \end{pmatrix} \mathbf{E} + \begin{pmatrix} p \\ n \end{pmatrix} \mathbf{u} \right] - D\nabla^2 \begin{pmatrix} p \\ n \end{pmatrix} = k_r \left(n_{eq}^2 F(\omega) - pn \right) \tag{4}$$

Here, the assumption of thermodynamic equilibrium for free charges is utilized to relate the dissociation rate to recombination rate, $k_d N = k_r n_{eq}^2$ where n_{eq} stands for the charge density at equilibrium. Finally, with d, $u_{\mathrm{ehd}} = b_+ V/d$, $\mu^2/\rho d^2$, V/d, and n_{eq}, respectively as scaling parameters for length, velocity, pressure, electric field, and free charges, one can obtain the nondimensional equations governing the system as follows:

$$\nabla \cdot \mathbf{u}^* = 0 \tag{5}$$

$$\begin{aligned} (\mathbf{u}^* \cdot \nabla)\,\mathbf{u}^* &= -\left(\frac{1}{\mathrm{Re}_{\mathrm{ehd}}}\right)^2 \nabla P^* \\ &+ \frac{1}{\mathrm{Re}_{\mathrm{ehd}}} \nabla^2 \mathbf{u}^* + M^2 C_0 \left(p^* - n^*\right) \mathbf{E}^* \end{aligned} \tag{6}$$

$$\nabla \cdot \mathbf{E}^* = \frac{1}{1 + \left(\frac{1}{b_r}\right)} C_0 \left(p^* - n^*\right), \qquad \mathbf{E}^* = -\nabla\phi^* \tag{7}$$

TABLE II
SUMMARY OF ELECTROSTATIC AND FLOW BOUNDARY CONDITIONS

HV electrode	Ground electrode	Liquid/solid interface	Inlet/outlet	Channel outer wall
$\mathbf{u}^*=0$			$\mathbf{n}\cdot\nabla\mathbf{u}^*\|_{in}=\mathbf{n}\cdot\nabla\mathbf{u}^*\|_{out}$, $\mathbf{u}^*\|_{in}=\mathbf{u}^*\|_{out}$	-
$\phi^*=1$	$\phi^*=0$	$\phi^*=\phi_s^*$	$\mathbf{n}\cdot\nabla\phi^*\|_{in}=\mathbf{n}\cdot\nabla\phi^*\|_{out}$, $\phi^*\|_{in}=\phi^*\|_{out}$	$\phi^*=0$
$p^*=0$, $\mathbf{n}\cdot\nabla n^*=0$	$n^*=0$, $\mathbf{n}\cdot\nabla p^*=0$	$\mathbf{n}\cdot\nabla(p^*,n^*)=0$	$\mathbf{n}\cdot\nabla(p^*,n^*)\|_{in}=\mathbf{n}\cdot\nabla(p^*,n^*)\|_{out}$, $(p^*,n^*)\|_{in}=(p^*,n^*)\|_{out}$	-

$$\nabla\cdot\left[\begin{pmatrix}p^*\\-n^*\end{pmatrix}\mathbf{E}+\begin{pmatrix}p^*\\b_rn^*\end{pmatrix}\mathbf{u}\right]-\alpha\nabla^2\begin{pmatrix}p^*\\b_rn^*\end{pmatrix}=\begin{pmatrix}C_0\\b_rC_0\end{pmatrix}(F(\omega)-p^*n^*) \quad (8)$$

where Langevine's approximation for dielectric fluids [13] is used to relate the recombination constant to the liquid properties; that is: $k_r=\frac{b_++b_-}{\epsilon}$. The resulting dimensionless coefficients in the above equations are defined as follows:

$$\mathrm{Re_{ehd}}=\frac{b_+V}{\nu},\quad M=\sqrt{\frac{\epsilon}{\rho{b_+}^2\left(1+\frac{1}{b_r}\right)}},$$
$$C_0=\frac{\sigma d^2}{b_+\epsilon V},\quad \alpha=\frac{D}{b_+V}=\frac{k_BT}{eV},\quad b_r=\frac{b_+}{b_-}$$

with the charge concentration at equilibrium, n_{eq}, defined as $n_{eq}=\frac{\sigma}{b_++b_-}$. The liquid is in contact with the channel wall which is assumed to be solid a insulator. Therefore, with no volumetric electric charges within the solid zone, the Laplace equation governs the potential field:

$$\nabla^{*2}\phi_s^*=0 \quad (9)$$

The boundary conditions are presented in Table II. Note that the continuity of potential field is applied across the solid/liquid interface where the liquid is in contact with the wall while the channel outer surface is grounded. No boundary condition is required for velocity and electric charges inside the solid wall since the corresponding equations are not solved within the solid zone. In addition, the zero flux boundary condition for electric charges across the solid/liquid interface is based on the negligibly small double layer thickness which implies that no charges cross the solid/liquid interface as the volumetric electric charge inside the solid zone is assumed to be zero. In addition, boundary conditions on the electrodes surfaces imply that charges with the same polarity as the electrodes do not accumulate on the surface of the electrodes while no diffusion of the charges with opposite sign exists right at the surface of the electrode. However, there exists charge diffusion in the upper layers within the heterocharge layer.

III. RESULTS AND DISCUSSIONS

The results presented in this section illustrate the role of charge mobility on the performance of EHD conduction pump. The reference values selected to calculate the dimensionless parameters and $br = 1$ correspond to the properties of refrigerant R-123 as the working fluid [2]. The values of the dimensionless numbers for the base case are presented in Table III and applied voltage of 10kV. Note that the values presented in this paper for b_r has been arbitrarily selected due to the lack of measured mobility ratios especially for refrigerant R-123. These results are presented to solely illustrate the effects of charges mobility on the generated flow.

TABLE III
NUMERICAL VALUES OF DIMENSIONLESS NUMBERS FOR THE BASIC CASE

Dimensionless number	Numeric value
$\mathrm{Re_{ehd}}$	1380
C_0	0.011
α	10^{-6}
b_r	1.0
	2.0
M	4.39
	3.58

First we examine the impact of charge mobility for symmetric electrodes configuration where no flow is expected when the mobility of positive and negative charges is identical. Later in this section, the role of charge mobility for asymmetric electrodes is investigated where net flow is generated due to the electrodes asymmetry in the case of identical mobilities. In addition, the variation of net generated flow over the range of mobility ratios for all electrodes configurations is presented and analyzed. Note that this range

A. Symmetric Electrodes Configuration

The results of electric field, net charge density and electric body force for symmetric electrodes configuration and identical mobility for positive and negative charges are presented in Fig. 2. The electrodes symmetry results in symmetric distribution of electric field and thus, net charge density. In addition, the inter-electrode region is characterized by high intensity electric field (see Fig. 2a) which yields in higher charge density in this region (Fig. 2b). Therefore, the resultant electric body force distribution is identical but in opposite directions above the electrodes surfaces. The flow streamlines presented in Fig. 3 confirm zero net generated flow which, of course, is associated with local flow circulations due to the local body force distribution.

The symmetric distribution of charges over the surfaces of identical electrodes will be broken once different mobilities are assigned for positive and negative charges. This mechanism along with the distribution of resultant electric body force is illustrated in Fig. 4 for $b_r = 2$. Note that this value of mobility ratio has not been specifically measured for R-123 but has been arbitrarily chosen by considering the measurement by Casanovas et. al [10] for purified silicon oil containing $\mathrm{C_7F_{14}}$. Here, negative charges have smaller mobility coefficient than the positive charges. Therefore, there exists more tendency for positive charges to migrate toward the electrodes due to the external electric field as governed by Eq. (8). The consequence is higher positive charge density on the surface of the ground electrode as observed in Fig. 4a which results in the dominance

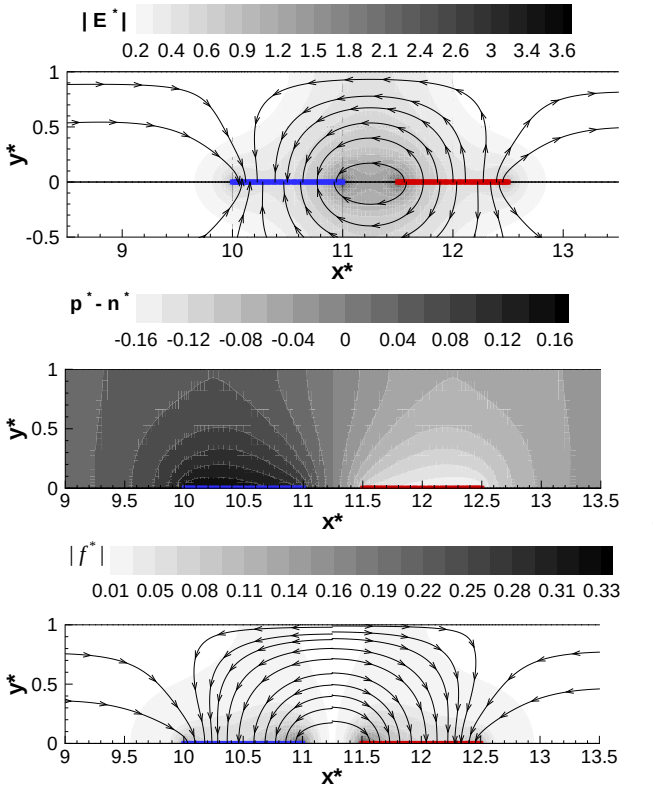

Fig. 2. Dimensionless contours of (a) electric field, (b) net charge density, and (c) electric body force with $b_r = 1$ and $\xi_r = 1$.

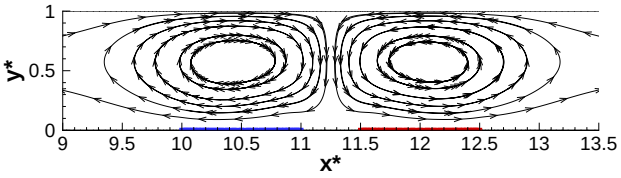

Fig. 3. Flow streamlines with $b_r = 1$ and $\xi_r = 1$.

of electric body force directing toward negative x-direction (see Fig. 4b). The flow streamlines displayed in Fig. 5 illustrate the net flow motion toward negative x-direction.

The variation of net generated flow with mobility ratio for different electrodes spacings is presented in Fig. 6. The dimensionless flow rate at the channel outlet is defined as:

$$Q^*_{\text{net}} = \frac{1}{u_{\text{ehd}} d} \int_0^d u_{\text{out}} dy \tag{10}$$

The generated flow initially increases and eventually drops with the mobility ratio. This scenario can be explained as follows: The initial increase in the generated flow is due to the more pronounced asymmetric charge distribution over the electrodes surfaces. However, larger values of mobility ratio suppress the migration of negative charges toward the HV electrode surface to yield lower charge density over the electrode surface as illustrated in Fig. 7. In addition, the electric field has a more uniform distribution around the ground electrode since charges tend to have a unipolar distribution on the surface of the ground electrode as the heterocharge layer on the HV electrode is inclined to disappear. Therefore, the two edges of the ground electrode are characterized by high intensity

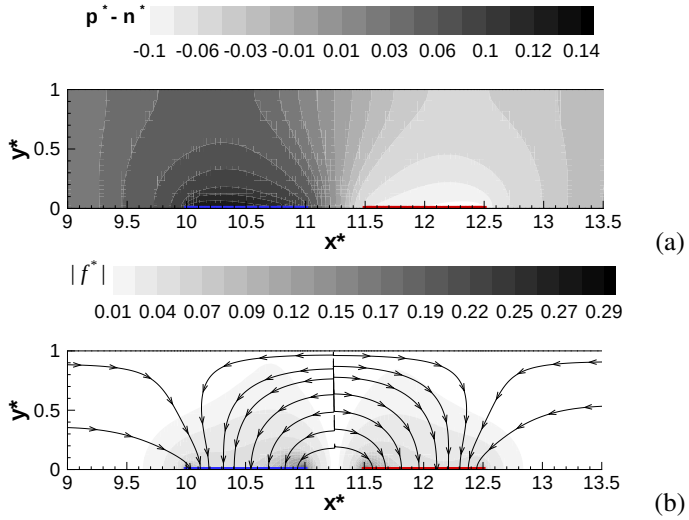

Fig. 4. Dimensionless contours of (a) net charge density and (b) electric body force with $b_r = 2$ and $\xi_r = 1$.

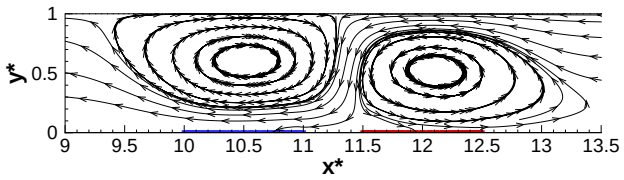

Fig. 5. Flow streamlines with $b_r = 2.$ and $\xi_r = 1$

electric body force in opposite directions as presented in Fig. 7, which adversely impact the generated liquid flow. Also shown in Fig. 6 is the effect of electrode gap on the generated flow. The flow is expected to increase as the electrode gap is reduced due to the higher electric filed intensity within the inter-electrode region.

B. Asymmetric Electrodes Configuration

The fundamental application of EHD conduction driven flow is based on the asymmetric electrodes geometry. As illustrated in Fig. 8, the consequence of electrodes asymmetry

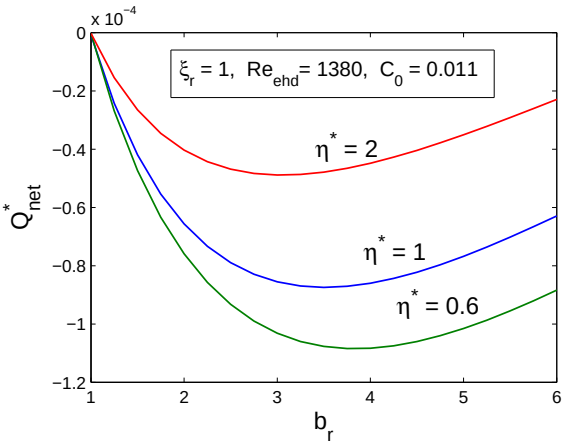

Fig. 6. Variation of net generated flow with mobility ratio for symmetric electrodes, $\xi_r = 1$.

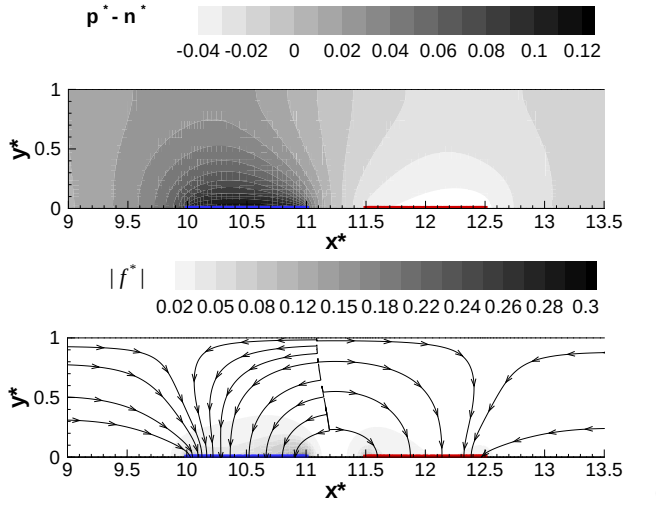

Fig. 7. Dimensionless contours of (a) net charge density and (b) electric body force with $b_r = 6$ and $\xi_r = 1$.

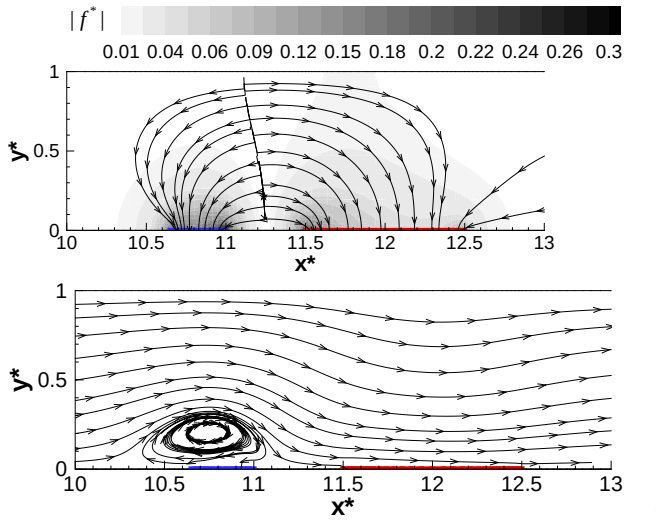

Fig. 8. (a) dimensionless electric body force contours and (b) flow streamlines with $\xi_r = 0.35$ and $b_r = 1$.

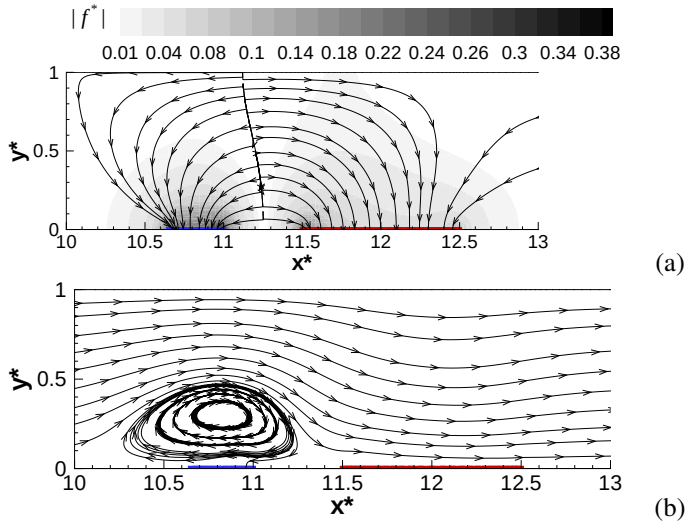

Fig. 9. (a) dimensionless electric body force contours and (b) flow streamlines $\xi_r = 0.35$ and $b_r = 2$.

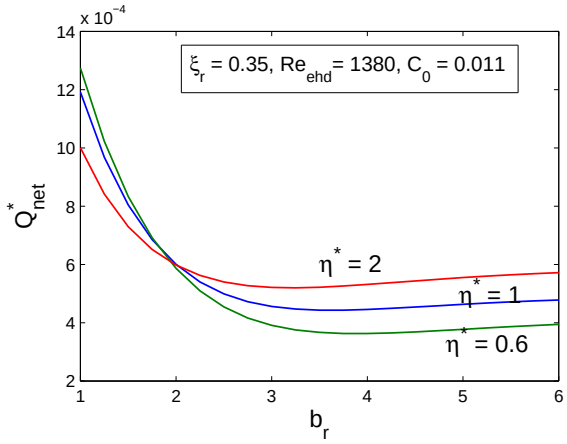

Fig. 10. Variation of net generated flow with mobility ratio for Asymmetric electrodes, $\xi_r = 0.35$.

is the dominance of the electric body force directed toward the broken symmetry; from the narrower electrode toward the wider electrode causing the net flow generated from left to the right of the channel. However, the presence of opposing electric body force results in local reversed flow which remains limited to the region close to the electrodes.

The impact of unequal mobility coefficients for positive and negative charges on the electric body force and flow field for $\xi_r = 0.35$ is depicted in Fig. 9. As discussed earlier, with $b_r > 1$, the positive charge density over the surface of the ground electrode surpasses the negative charge density over the HV electrode. For the given configuration, this will enhance the opposing body force on the edge of the ground electrode to increase the circulating flow (see Fig. 9b) and lower the generated flow.

Figure 10 presents the variation of generated flow with mobility ratio. The immediate drop of the flow rate for $b_r > 1$ is due to the increase in the opposing electric body force on the edge of the narrower (ground) electrode. However, the course is eventually reversed for larger values of mobility ratios per our earlier discussion. Noticeably, the upward trend starts at smaller mobility ratios and leads to a slightly larger flow rate for large mobility ratios when the gap between the electrodes expands. This is because the electric field encounters less variation across the electrodes edges when the gap is larger yielding in earlier transition to "pseudo-unipolar" charge distribution over the electrode surface.

Finally, before concluding this study, we present the variation of net flow with mobility ratio for the case of $\xi_r = 2.86$ where the broken symmetry requires the flow to be generated from right to the left. As observed in Fig. 11, the flow increases with the mobility ratio as the direct consequence of promoted body force on the right edge of the ground electrode. However, the transition to a symmetric distribution over the electrode surface occurs at much larger mobility ratios since the mobile charge carriers are now migrating toward the wider electrode. The threshold at which the trend shifts is seen to occur far beyond $b_r = 6$ and therefore is not presented here.

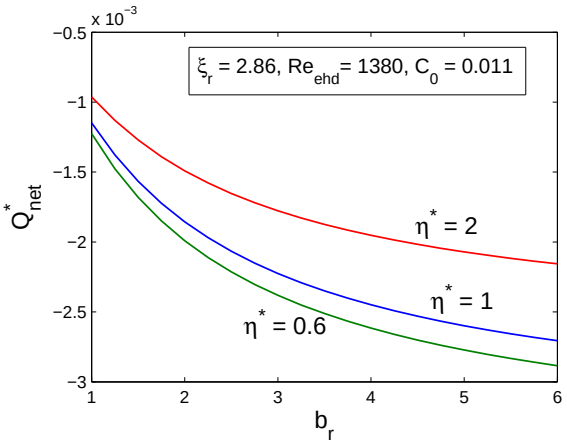

Fig. 11. Variation of net generated flow with mobility ratio for asymmetric electrodes, $\xi_r = 2.86$.

IV. CONCLUSIONS

The effect of unequal mobility ratios of positive and negative charge carriers ($b_r = b_+/b_- > 1$) on the performance of EHD conduction pumping was investigated. Net flow was observed for the case of symmetric electrodes and $b_r > 1$ which is attributed to the non-symmetric charge distribution over the electrodes. The net flow decreased for large mobility ratios as the migration of negative charges is suppressed to result in relatively uniform charge and body force distribution over the surface of ground electrode. The impact of charge mobility for asymmetric electrodes was analyzed as well. With $b_r > 1$, the flow was adversely impacted compared to the case of identical mobilities when it was generated from the ground electrode toward the HV electrode, but it was positively affected by the unequal mobility coefficients when it was generated from the HV electrode toward the ground electrode.

ACKNOWLEDGMENT

This work was financially supported by the NASA Microgravity Fluid Physics Program.

REFERENCES

[1] J. Seyed-Yagoobi, "Electrohydrodynamic pumping of dielectric liquids," *J. Electrostatics*, vol. 63, pp. 861–869, 2005.
[2] M. Yazdani and J. Seyed-Yagoobi, "Numerical investigation of electrohydrodynamic-conduction pumping of liquid film in the presence of evaporation," *ASME J. Heat Transfer*, vol. 131, 2008.
[3] Y. Feng and J. Seyed-Yagoobi, "Electrical charge transport and energy conversion with fluid flow during electrohydrodynamic conduction pumping," *Physics of Fluids*, vol. 19, no. 5, p. 057102, 2007.
[4] M. Yazdani and J. Seyed-Yagoobi, "Electrically induced dielectric liquid film flow based on electric conduction phenomenon," *IEEE. Trans. on Dielectric liquids, in press*, 2009.
[5] R. Hanaoka, I. Takahashi, S. Takata, T. Fukami, and Y. Kamamaru, "Properties of ehd pump with combination of rod-to-rod and meshy parallel plates electrode assemblies," *IEEE Trans. Dielectrics and Electrical Insulations*, vol. 16, no. 2, pp. 440–447, April 2009.
[6] P. S. Winokur, M. L. Roush, and J. Silverman, "Ion mobility measurements in dielectric liquids," *The Journal of Chemical Physics*, vol. 63, no. 8, pp. 3478–3489, 1975.
[7] S. Ishii, T. Aoki, M. Nagao, and M. Kosaki, "The mobility measurement of positive charge carrier in n-hexane," Oct 1994, pp. 854–859.
[8] S. S.-S. Huang and G. R. Freeman, "Positive ion mobilities in gaseous, critical, and liquid hydrocarbons: Density and temperature effects," *The Journal of Chemical Physics*, vol. 70, no. 3, pp. 1538–1543, 1979.
[9] S. Sakamoto and H. Yamada, "Optical study of conduction and breakdown in dielectric liquids," *Electrical Insulation, IEEE Transactions on*, vol. EI-15, no. 3, pp. 171–181, June 1980.
[10] J. Casanovas, R. Grob, A. Chemin, J. P. Guelfucci, and J.-P. Crine, "Ion mobility measurements in a 50 cst viscosity polydimethylsiloxane silicone oil," *Electrical Insulation, IEEE Transactions on*, vol. EI-20, no. 2, pp. 143–146, April 1985.
[11] P. Atten and J. Seyed-Yagoobi, "Electrohydrodynamically induced dielectric liquid flow through pure conduction in point/plane geometry," *IEEE Trans. Dielectr. Electr. Insul*, vol. 10, p. 23, 2003.
[12] S. I. Jeong, J. Seyed-Yagoobi, and P. Atten, "Theoretical/numerical study of electrohydrodynamic pumping through conduction phenomenon," *IEEE Trans. Dielectr. Electr. Insul*, vol. 39, p. 355, 2003.
[13] P. Langevin, "Recombmaison et mobilites des ions dans les gag," *Ann. Chim. Phys*, vol. 28, p. 433, 1903.